

Nighttime Image Dehazing Based on Variational Decomposition Model

Yun Liu¹, Zhongsheng Yan¹, Aimin Wu², Tian Ye³, Yuche Li^{4*}

¹College of Artificial Intelligence, Southwest University, Chongqing 400715, China

²College of Big Data & Intelligent Engineering, Chongqing College of International Business and Economics, Chongqing 401520, China

³School of Ocean Information Engineering, Jimei University, Xiamen, 361021, China

⁴College of Geosciences, China University of Petroleum, Beijing 102249, China

yunliu@swu.edu.cn, zhongshengyanzy@foxmail.com, 3064469096@qq.com, 201921114031@jmu.edu.cn,

liyuche_cq@163.com

Abstract

Most of existing dehazing algorithms are unable to deal with nighttime hazy scenarios well due to complex degraded factors such as non-uniform illumination, low light and glows. To obtain high-quality image under nighttime haze imaging conditions, we present an effective single nighttime image dehazing framework based on a variational decomposition model to simultaneously address these undesirable issues. First, a variational decomposition model consisting of three regularization terms is proposed to simultaneously decompose a nighttime hazy image into a structure layer, a detail layer and a noise layer. Concretely, we employ ℓ_1 norm to constrain the structure component, adopt ℓ_0 sparsity term to enforce the piece-wise continuous of the detail layer, and use ℓ_2 norm to separate the noise layer. Next, the structure layer is recovered by means of inverting the physical model and the detail layers are revealed in a multi-scale gradient enhancement manner. Finally, the dehazed structure layer and the enhanced detail layers are integrated into a haze-free image. Experimental results show that the proposed framework achieves superior performance on nighttime haze removal and noise suppression compared with several state-of-the-art dehazing techniques.

1. Introduction

In contrast to daytime haze imaging conditions, the nighttime illumination is dominated by active, artificial light sources such as street and neon lights and these lights may have low illumination and yield diverse colors. Therefore, outdoor images or videos acquired under nighttime hazy scenes usually are affected by more complex degraded factors such as haze interference, texture blurring, glow effects, color distortion and noise disturbance. To ensure the

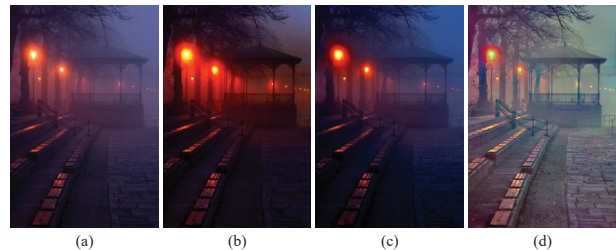


Figure 1. (a) Input nighttime hazy image. (b)-(d) are dehazing results generated by DCP [10], MSCNN [30] and ours respectively. Daytime dehazing methods fail to deal with nighttime hazy scenes.

performance of outdoor computer vision applications under nighttime hazy scenarios, it is significant to develop specialized dehazing algorithm for nighttime hazy images.

To the best of our knowledge, great achievements have been made in the field of daytime image dehazing over the past decades. Most of existing daytime dehazing algorithms can be divided into two categories: prior-based methods [3, 4, 8, 10, 13, 14, 42] and learning-based methods [5–7, 18, 19, 28–32, 34, 36]. Despite achieving pleasant results at daytime scenes, these methods are not capable of improving the quality of nighttime hazy images, depicted in Fig. 1. This is due to the fact that there exists differences on degradation characteristics between nighttime hazy images and daytime hazy images.

To circumvent this challenging issue, some works have been devoted to propose dehazing techniques focusing on nighttime hazy images. Pei and Lee [27] make use of a color transfer method to convert the airlight color from a “blue shift” to a “grayish” by referring to the color characteristics of a daytime hazy image. After mitigating the color distortion, they further adopt traditional prior-based dehazing strategy to remove the haze. Considering the non-uniform illumination from artificial light sources, Zhang *et al.* [40] modified the atmospheric scattering model [17] by replacing the constant atmospheric light with pointwise variables

*Corresponding author.

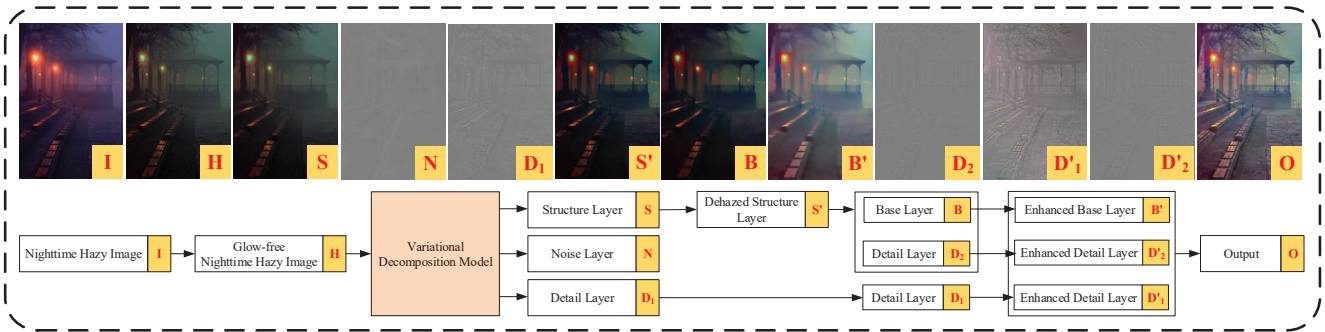


Figure 2. Overview of proposed nighttime image dehazing framework.

for achieving light compensation, color correction and haze removal. To diminish the glow effects, the glow layer is removed in [21] by using relative smoothness constraints. Base on a new imaging model [40], Zhang *et al.* [39] develop the maximum reflection prior to estimate key parameters, and consequently produce a haze-free image. Meanwhile, a faster approximated parameters estimation method is also given in [39]. From the viewpoint of image fusion, Yu *et al.* [38] introduce a pixel-wise alpha blending method to estimate model-based parameters. In [41], Zhang *et al.* generate the first synthetic nighttime hazy images benchmark dataset and also provide a optimal-scale fusion method to remove the color cast and nighttime haze.

Although these above methods can improve the performance of nighttime hazy images in visibility, colors and noise suppression, they fail to consider the noise amplification in the process of nighttime image dehazing and provide a comprehensive nighttime image dehazing solution. In summary, existing nighttime dehazing techniques have following problems:

Visual quality: The overall visual quality of recovered results generated by existing approaches is unnatural and limited because these methods only consider partial degradation factors such as color distortion, glow effects and nighttime haze. For instance, Li *et al.* [21] only take the glows and nighttime haze into account but ignore the brightness adjustment. Similarly, the glow effects from multiple artificial light sources are also neglected in [39, 40]. Owing to these issues, existing methods may have limited performance of the visual quality.

Noise suppression: Noise is an inevitable factor in real-world nighttime hazy scenarios, which will be amplified in the process of enhancement or restoration. Because existing enhancement methods cannot effectively distinguish the details and noises of the nighttime hazy images, the hidden noises will be amplified while details enhancement. For the restoration methods, the problem of noise amplification is especially obvious for the regions with lower transmission $t(x)$ due to dividing by $t(x)$ in the process of model inverting. Therefore, noise suppression should be conducted

while nighttime image dehazing.

To compensate for the aforementioned deficiencies, in this paper, we propose a multi-purpose oriented single nighttime image dehazing framework which can simultaneously handle multiple degradation factors such as glow effects, color distortion, brightness adjustment, haze interference, detail blurring, noise amplification and so on. The main contributions of this paper are summarized as follows:

- We fully consider multiple degradation factors of nighttime hazy scenes and develop a comprehensive single nighttime dehazing solution to produce a high-quality haze-free image with more details and less noises. Experiments demonstrate the proposed framework outperforms several state-of-the-art specialized dehazing techniques.
- A variational decomposition model is proposed to decompose a nighttime hazy image into a structure layer, a detail layer and a noise layer. Specifically, the proposed model includes three hybrid regularization terms namely ℓ_1 - ℓ_0 - ℓ_2 norm to enforce the structure part, the detail part and the noise part, respectively, which can differentiate the details and the noises well.
- In order to further enhance the details and suppress the noises simultaneously, the multi-scale decomposition strategy is used in the proposed framework. Concretely, we further decompose the dehazed structure layer into a base layer and a detail layer and set different coefficients to enhance two detail layers with different attributes in the gradient domain, which can suppress the amplified noises in the process of structure dehazing while enhancing the details.

2. Related Work

According to the dominate imaging light sources, existing dehazing approaches are roughly divided into two categories: daytime dehazing methods [3–8, 10, 13, 14, 18, 19, 24, 28–32, 34, 36, 42] and nighttime dehazing methods [1, 2, 21, 23, 26, 27, 37–41].

Daytime Dehazing Methods: Early dehazing methods [3, 4, 8, 10, 13, 14, 42] usually rely on the atmospheric scattering model and the hand-crafted priors to estimate the unknown parameters, namely the transmission $t(x)$ and the atmospheric light A . For example, He *et al.* [10] develop a novel prior called dark channel prior (DCP) based on the statistical analysis of massive outdoor haze-free images. Using this prior, the physical model is inverted to obtain the clean image. Subsequently, some effective human-selected priors are presented for recovering haze-free images such as color-lines [8], color attenuation prior [42], haze-lines [3], color ellipsoid prior [4], region line prior [13] and more. However, these prior-based methods may not always hold in case of the complex real-world hazy scenes. To overcome hand-designed priors dependency, numerous deep learning based dehazing networks [5–7, 18, 19, 28–32, 34, 36] are proposed to learn the mapping relationship from hazy images to unknown parameters or haze-free images. DehazeNet [5] and MSCNN [30] are first devised to predict the transmission and then the haze-free images can be acquired by substituting the estimated parameters provided by dehazing networks into the atmospheric scattering model. Li *et al.* [18] present an all-in-one dehazing network dubbed as AOD-Net that learns $t(x)$ and A jointly through a designed K estimation module, which achieves haze removal in an end-to-end fashion. Afterwards, various end-to-end dehazing networks, such as GFN [31], PDN [36], FFA-Net [28], MSBDN [7] DA-Net [32], PSD-Net [6] and more, have been developed to directly learn hazy-to-clear image translation. All of these aforementioned methods can handle daytime hazy images well, but they show limited capability of improving performance for nighttime hazy images, as depicted in Fig. 1. This is because that the nighttime hazy images are deteriorated by multiple degraded factors (non-uniform illumination, haze interference, low-light, glow effects, etc.) compared with daytime hazy images and the classic atmospheric model cannot explain these degraded features.

Nighttime Dehazing Methods: To our knowledge, less progress on nighttime dehazing has been made than daytime dehazing. Pei and Lee [27] exploit the color transfer technology to convert the airlight color from a “bluish” to a “grayish” and adopt the DCP to remove the nighttime haze. However, this method usually needs a reference image for color transfer, which is not well-suited for real applications. From the viewpoint of image fusion, Ancuti *et al.* [1] devise a multi-scale fusion approach to enhance nighttime hazy images through using several inputs derived from the input image. Taking the non-uniform imaging light sources into account, a patch-based method [2] is presented for atmospheric light estimation. Yu *et al.* [38] propose a pixel-wise alpha blending fusion method to estimate the transmission map. Nevertheless, the noises are amplified in the

results obtained by fusion-based while enhancing the nighttime hazy images. Starting from the perspective of model-based, Zhang *et al.* [40] build a new imaging model for nighttime haze condition considering the degraded factors caused by non-uniform artificial light sources and conduct light compensation and color correction prior to dehazing. This method can improve the contrast of the nighttime hazy image, but the results look unnatural. Based on this model, a prior called maximum reflectance prior (MRP) is devised to estimate the ambient illumination. Li *et al.* [21] take the glow effects into account and add a glow term into the traditional atmospheric scattering model. Leveraging the decomposition strategy, Liu *et al.* [23] devise a linear model to describe four parts of a nighttime hazy image and then propose a weighted- ℓ_2 energy function to separate the use-less noises and glows. More recently, deep learning based networks [16, 41] are proposed for solving the problem of nighttime image dehazing. For instance, Koo *et al.* [16] propose a glow-decomposition network based on the generative adversarial network to alleviate the glow effects. Zhang *et al.* [41] develop a synthetic benchmark and an encoder-decoder architecture consisting of a MobileNetv2 backbone as the encoder and a fully convolution decoder for removing the nighttime haze. In summary, these above specialized nighttime dehazing methods fail to provide a comprehensive solution for nighttime image dehazing.

3. Proposed Method

On the basis of the linear decomposition model [23], a nighttime hazy image $I(x)$ can be described as a linear combination of four parts: a structure layer $S(x)$, a detail layer $D(x)$, a noise layer $N(x)$ and a glow layer $G(x)$:

$$I(x) = S(x) + D(x) + N(x) + G(x) \quad (1)$$

To correct color distortions and alleviate glow effects prior to dehazing, the glow term is first removed based on the method [21] to acquire the glow-free image \mathbf{H} .

3.1. Variational Decomposition Model

After glow removal, we propose a variational decomposition model consisting of hybrid ℓ_0 - ℓ_1 - ℓ_2 norm regularization terms to simultaneously estimate the structure \mathbf{S} , the detail \mathbf{D} and the noise \mathbf{N} . The matrix-vector formulation of the energy optimization function is expressed as follows:

$$\arg \min_{\mathbf{S}, \mathbf{D}, \mathbf{N}} \|\mathbf{S} + \mathbf{D} + \mathbf{N} - \mathbf{H}\|_2^2 + \alpha \|\nabla \mathbf{S}\|_1 + \beta \|\nabla \mathbf{D} - \nabla \mathbf{H}\|_0 + \delta \|\mathbf{N}\|_2^2 \quad (2)$$

where α , β and δ are positive that control the balance of different regularization terms, $\|\cdot\|_p$ denotes the p -norm and ∇ represents first-order differential operator. In (2), the first

term is the data fidelity term that constrains the distance between the estimated $\mathbf{S} + \mathbf{D} + \mathbf{N}$ and \mathbf{H} and the second term considers the piece-wise smoothness of the structure part. The third term enforces the non-zero gradients between \mathbf{D} and \mathbf{H} at the same position for preserving structural edges. The overall noise intensity is constrained in the last term for noise suppression.

The main contribution of the proposed variational model is to use hybrid regularization terms in a unified way, resulting in providing a structure layer, a structure-aware detail layer and a noise layer effectively. Specifically, owing to the excellent effectiveness of ℓ_0 gradient sparsity constraint in edge preserving [35], tone mapping [22] and low-light enhancement [12], we employ it to constrain non-zero gradients of \mathbf{D} and \mathbf{H} for acquiring structural edges of the input image and reducing tiny edges, which is conducive to distinguishing the details and noises and further achieving noise suppression while enhancing details.

3.2. Numerical Solver

To solving the non-convex optimization problem (2), we substitute two auxiliary variables \mathbf{T} and \mathbf{L} into (2) and the objective function can be rewritten as follows:

$$\begin{aligned} \arg \min_{\mathbf{S}, \mathbf{D}, \mathbf{N}} \|\mathbf{S} + \mathbf{D} + \mathbf{N} - \mathbf{H}\|_2^2 + \alpha \|\mathbf{T}\|_1 + \beta \|\mathbf{L}\|_0 + \delta \|\mathbf{N}\|_2^2 \\ \text{s.t. } \mathbf{T} = \nabla \mathbf{S}, \mathbf{L} = \nabla \mathbf{D} - \nabla \mathbf{H} \end{aligned} \quad (3)$$

Then, two Lagrange multipliers \mathbf{Z}_1 and \mathbf{Z}_2 are introduced for removing the equality constraint and we can have:

$$\begin{aligned} \mathcal{L}(\mathbf{S}, \mathbf{D}, \mathbf{N}, \mathbf{T}, \mathbf{L}, \mathbf{Z}_1, \mathbf{Z}_2) = \|\mathbf{S} + \mathbf{D} + \mathbf{N} - \mathbf{H}\|_2^2 \\ + \alpha \|\mathbf{T}\|_1 + \beta \|\mathbf{L}\|_0 + \delta \|\mathbf{N}\|_2^2 \\ + \Phi(\mathbf{Z}_1, \mathbf{T} - \nabla \mathbf{S}) + \Phi(\mathbf{Z}_2, \mathbf{L} - \nabla \mathbf{D} + \nabla \mathbf{H}) \end{aligned} \quad (4)$$

where $\Phi(\mathbf{A}, \mathbf{B}) = \langle \mathbf{A}, \mathbf{B} \rangle + \frac{\mu}{2} \|\mathbf{B}\|_2^2$ and $\langle \cdot, \cdot \rangle$ stands for the matrix inner product. The objective function (4) can be solved by updating each variable iteratively while fixing other variables. Next, we give the solutions for each sub-problem at k -th iteration.

S sub-problem: Collecting the terms related to \mathbf{S} , we can have the following objective function:

$$\arg \min_{\mathbf{S}} \|\mathbf{S} + \mathbf{D}^k + \mathbf{N}^k - \mathbf{H}\|_2^2 + \Phi(\mathbf{Z}_1^k, \mathbf{T}^k - \nabla \mathbf{S}) \quad (5)$$

By solving the classic least squares problem (5), \mathbf{S}^{k+1} can be calculated using 2D FFT techniques:

$$\mathbf{S}^{k+1} = \mathcal{F}^{-1} \left(\frac{2\mathcal{F}(\mathbf{H} - \mathbf{D}^k - \mathbf{N}^k) + \mu^k \mathbf{M}_1}{2 + \mu^k \sum_{d \in \{h, v\}} \mathcal{F}^*(\mathbf{G}_d) \circ \mathcal{F}(\mathbf{G}_d)} \right) \quad (6)$$

where $\mathbf{M}_1 = \sum_{d \in \{h, v\}} \mathcal{F}^*(\mathbf{G}_d) \circ \mathcal{F}(\mathbf{T}^k + \mathbf{Z}_1^k / \mu^k)$ and \mathbf{G} represents the discrete gradient operator, containing \mathbf{G}_h and

\mathbf{G}_v . In addition, $\mathcal{F}(\cdot)$ is 2D FFT operator, $\mathcal{F}^{-1}(\cdot)$ and $\mathcal{F}^*(\cdot)$ are the 2D inverse FFT and complex conjugate of $\mathcal{F}(\cdot)$, respectively. The operator “ \circ ” performs in a pixel-wise multiplication manner.

D sub-problem: Ignoring the terms unrelated to \mathbf{D} , the objective function (4) becomes:

$$\arg \min_{\mathbf{D}} \|\mathbf{S}^{k+1} + \mathbf{D} + \mathbf{N}^k - \mathbf{H}\|_2^2 + \Phi(\mathbf{Z}_2^k, \mathbf{L}^k - \nabla \mathbf{D} + \nabla \mathbf{H}) \quad (7)$$

Similarly, we solve (7) by differentiating it with regard to \mathbf{D} and setting it to 0:

$$\mathbf{D}^{k+1} = \mathcal{F}^{-1} \left(\frac{2\mathcal{F}(\mathbf{H} - \mathbf{S}^{k+1} - \mathbf{N}^k) + \mu^k \mathbf{M}_2}{2 + \mu^k \sum_{d \in \{h, v\}} \mathcal{F}^*(\mathbf{G}_d) \circ \mathcal{F}(\mathbf{G}_d)} \right) \quad (8)$$

where $\mathbf{M}_2 = \sum_{d \in \{h, v\}} \mathcal{F}^*(\mathbf{G}_d) \circ \mathcal{F}(\mathbf{L}^k + \nabla \mathbf{H} + \mathbf{Z}_2^k / \mu^k)$.

N sub-problem: Dropping the terms unrelated to \mathbf{N} , \mathbf{N}^{k+1} can be solved as follows:

$$\mathbf{N}^{k+1} = (\mathbf{H} - \mathbf{S}^{k+1} - \mathbf{D}^{k+1}) / (1 + \delta) \quad (9)$$

T sub-problem: Neglecting the terms irrelevant to \mathbf{T} , we can obtain:

$$\arg \min_{\mathbf{T}} \alpha \|\mathbf{T}\|_1 + \Phi(\mathbf{Z}_1^k, \mathbf{T} - \nabla \mathbf{S}^{k+1}) \quad (10)$$

Then, we perform the shrinkage operation to achieve the closed form solution of (10):

$$\mathbf{T}^{k+1} = \mathcal{T}_{\beta / \mu^k}(\nabla \mathbf{S}^{k+1} - \mathbf{Z}_1^k / \mu^k) \quad (11)$$

where $\mathcal{T}_t(x) = \text{sign}(x) \max(|x| - t, 0)$.

L sub-problem: Collecting the \mathbf{L} involved terms from (4) leads to the following optimization problem:

$$\arg \min_{\mathbf{L}} \beta \|\mathbf{L}\|_0 + \Phi(\mathbf{Z}_2^k, \mathbf{L} - \nabla \mathbf{D}^{k+1} + \nabla \mathbf{H}) \quad (12)$$

By analyzing [22, 35], we can optimize the above function (12) in a pre-entry fashion and the solution of \mathbf{L}_j^{k+1} at entry j is formulated as follows:

$$\mathbf{L}_j^{k+1} = \begin{cases} 0, & \text{if } (\mathbf{R}_j^k)^2 \leq 2\beta / \mu^k \\ \mathbf{R}_j^k, & \text{otherwise} \end{cases} \quad (13)$$

where $\mathbf{R}_j^k = (\nabla \mathbf{D}^{k+1} - \nabla \mathbf{H} - \mathbf{Z}_2^k / \mu^k)_j$, $j = 1, \dots, 2N$ and N stands for the total number of pixels within the image.

Updating $\mathbf{Z}_1, \mathbf{Z}_2$ and μ : The updating of parameters can be done through:

$$\begin{aligned} \mathbf{Z}_1^{k+1} &= \mathbf{Z}_1^k + \mu^k (\mathbf{T}^{k+1} - \nabla \mathbf{S}^{k+1}) \\ \mathbf{Z}_2^{k+1} &= \mathbf{Z}_2^k + \mu^k (\mathbf{L}^{k+1} - \nabla \mathbf{D}^{k+1} + \nabla \mathbf{H}) \\ \mu^{k+1} &= 2^2 \mu^k \end{aligned} \quad (14)$$

The entire iteration is stopped when the maximal number of iterations K is achieved ($K = 15$).

Algorithm 1 Solution of Proposed Model (2)

Input: pre-processed image \mathbf{H} , parameters α , β , and δ , maximum iterations K .

Initialization: $\mathbf{R}_0 = t_0(x)$, $\mathbf{N}_0 = \mathbf{0}$, $k = 0$.

- 1: **for** $k = 1$ to K **do**
- 2: Update \mathbf{S}^{k+1} using (6);
- 3: Update \mathbf{D}^{k+1} using (8);
- 4: Update \mathbf{N}^{k+1} using (9);
- 5: Update \mathbf{T}^{k+1} using (11);
- 6: Update \mathbf{L}^{k+1} using (13);
- 7: Update \mathbf{Z}_1^{k+1} , \mathbf{Z}_2^{k+1} and μ^k using (14);
- 8: **End**

Output: Final \mathbf{S}^k , \mathbf{D}^k , and \mathbf{N}^k .

3.3. Dehazing on Structure Layer

Because the research [15] have revealed that the hazes usually affect the low-frequency part of hazy images, we apply the dehazing operation for structure layer based on improved atmospheric scattering model. Considering the illumination dominated by artificial light sources, the constant atmospheric light is replaced with the spatially varying variable $A(x)$ and the restoration of structure layer is achieved by inverting the physical model:

$$S'(x) = \frac{S(x) - A(x)}{\max(t(x), t_0)} + A(x) \quad (15)$$

where the varying atmospheric light is assumed as the maximum pixel value locally and the transmission map is calculated based on dark channel prior [10] and guided image filtering [11].

3.4. Decomposition on Dehazed Structure Layer

To improve the nighttime dehazing results further, we make use of the decomposition model based on total variation [20] to provide a piece-wise smoothness base layer and a piece-wise constant detail layer. The base layer \mathbf{B} is obtained by solving the following optimization problem:

$$\arg \min_{\mathbf{B}} \|\mathbf{B} - \mathbf{S}'\|_2^2 + \lambda \|\nabla \mathbf{B}\|_1 \quad (16)$$

Then, the detail layer is computed by subtracting \mathbf{B} from \mathbf{S}' . To differentiate two detail layers from (2) and (16), we mark them as \mathbf{D}_1 and \mathbf{D}_2 , respectively.

By leveraging multi-scale scheme, different attributes of image details are captured into the corresponding layer and we control different amplification coefficients to handle them, which can not only improve prominent structures and enhance the fine details but also suppress the undesirable noises.

3.5. Multi-scale Enhancement

Due to the characteristics of poor illumination of the base layer, we apply the gamma correction (1/2.2) on the base layer to improve the brightness for highlight the structures. In addition, inspired by [9, 23, 25], two detail layers are enhanced by manipulating its gradient field without introducing halo artifacts. Usually, the mean transmission of a hazy image reflects its overall degradation degree and the smaller value of t leads to the lower visibility. Therefore, the reciprocal of the average transmission is considered as the enhancement coefficients and the manipulated gradients of each detail layer are as follows:

$$\nabla \mathbf{D}'_i = \frac{\omega_i}{\text{mean}(t)} \nabla \mathbf{D}_i \quad (17)$$

where $i = 1, 2$ and ω_i is the strength factor. From (15), we find that the tiny noises may be amplified in the process of dehazing especially for the region with the smaller t within the image and therefore the value of strength factor ω_2 is generally smaller than ω_1 for mitigating the noises. Empirically, we set ω_1 and ω_2 as 1.0 and 0.5, respectively.

Finally, the detail layers \mathbf{D}'_i are reconstructed by solving Poisson equation [9] and thus the nighttime dehazed output is obtained by:

$$\mathbf{O} = \mathbf{B}' + \mathbf{D}'_1 + \mathbf{D}'_2 \quad (18)$$

4. Experiments

In order to prove the effectiveness of the proposed framework, we compare it with several professional nighttime dehazing methods on real-world and synthetic images, including NDIM [40], GS [21], MRP [39], MRP_Faster [39], and OSFD [41]. GS [21], and our method are conducted using MATLAB R2019a and other methods are performed using the executable code from authors' website on a PC with Intel Core i5-8350U CPU and 16GB RAM. In the proposed framework, we empirically set the parameters α , β , δ and λ as 10^{-2} , 10^{-4} , 10^{-2} and 10^{-2} , respectively. For the color nighttime hazy images, the proposed variational decomposition model is employed for the V-channel in the HSV color space and then transform it back to the RGB color space.

4.1. Qualitative Comparisons on Real-world Images

As can be seen in Fig. 3, the details in the results provided by NDIM [40] are revealed, but they look unnatural and are vulnerable to the noises. GS [21] can mitigate the glow effects around artificial light sources and remove the nighttime haze. However, the ability of details recovery is insufficient. The results of MRP [39] and MRP_Faster [39] seem to be too dim and the details in the low light region are not recovered well. OSFD [41] severely suffers from

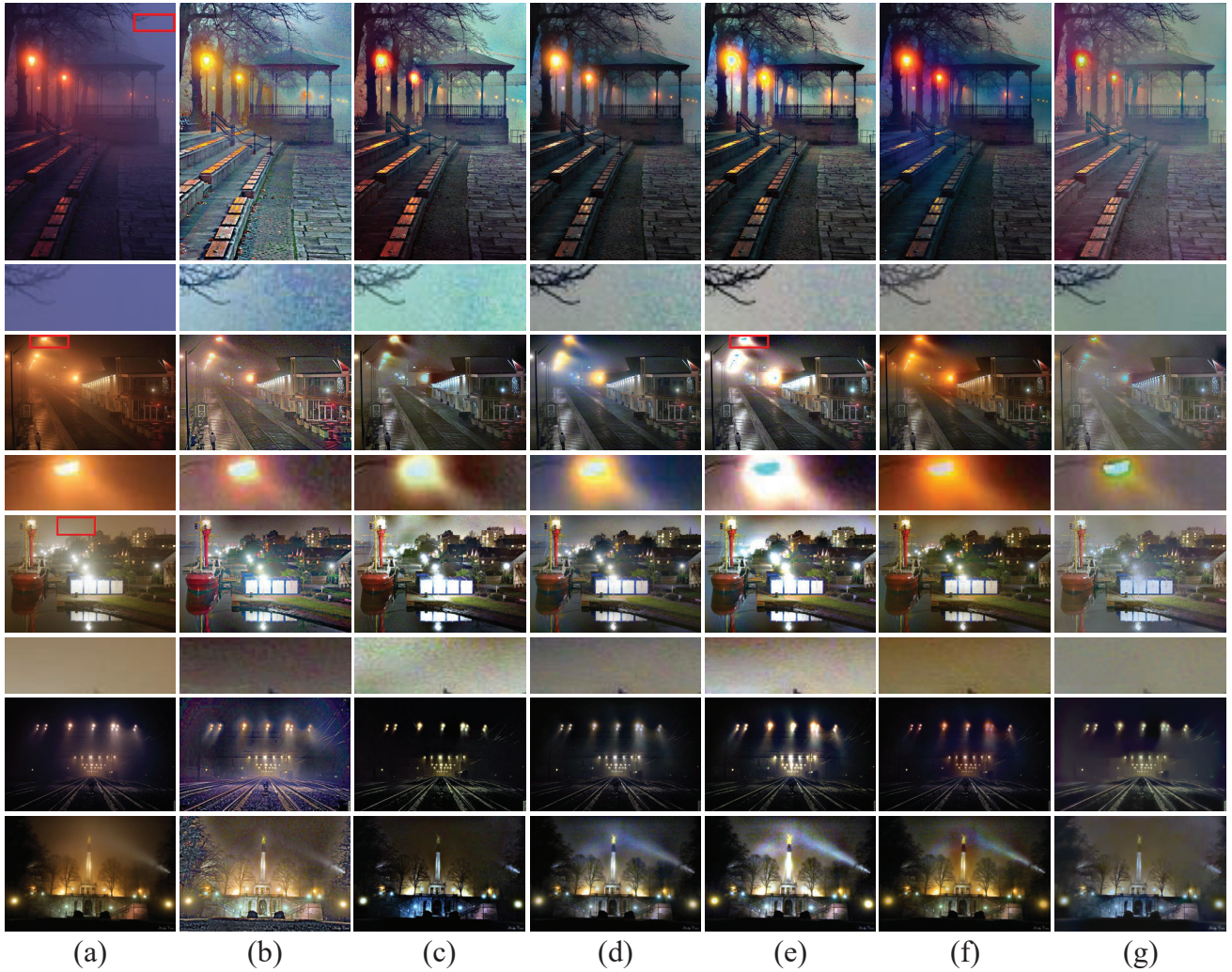


Figure 3. Comparisons of state-of-the-art nighttime dehazing methods on real-world scenes. (a) Nighttime hazy images. (b) NDIM [40]. (c) GS [21]. (d) MRP [39]. (e) MRP-Faster [39]. (f) OSFD [41]. (g) Ours.

glow effects around artificial light sources. In addition, the unwanted noises are also boosted in the results generated by five specialized approaches shown in the second and sixth row of Fig. 3. In comparison, the proposed framework achieves visually pleasant results in terms of details enhancement, noise suppression, illumination compensation and haze removal.

4.2. Quantitative Comparisons on Synthetic Images

To further verify the performance of the proposed framework, comparisons on synthetic images are also conducted. First, five representative synthetic examples with different haze thickness are selected from the latest released dataset called “Nighttime Hazy Middlebury”(NHM) [41] to facilitate the comparison, depicted in Fig. 4. From Fig. 4(b)-(h),

NDIM [40] can improve the visibility and contrast of nighttime hazy images to a great extent, whereas the dehazed results appear unnatural and uneven illumination. GS [21] is not capable of compensating the brightness and the results look too dim. MRP and MRP-Faster [39] can effectively remove the nighttime haze, but the glow effects nearby the light sources are not alleviated. The details are not recovered in the results yield by OSFD [41]. Moreover, the aforementioned methods suffer from noise amplification due to failing to consider the noise of nighttime hazy images, depicted in the second and last row of Fig. 4. Overall, these algorithms cannot provide a comprehensive solution for nighttime image dehazing. In contrast to their approaches, the proposed framework can simultaneously improve the contrast, compensate the brightness, suppress the

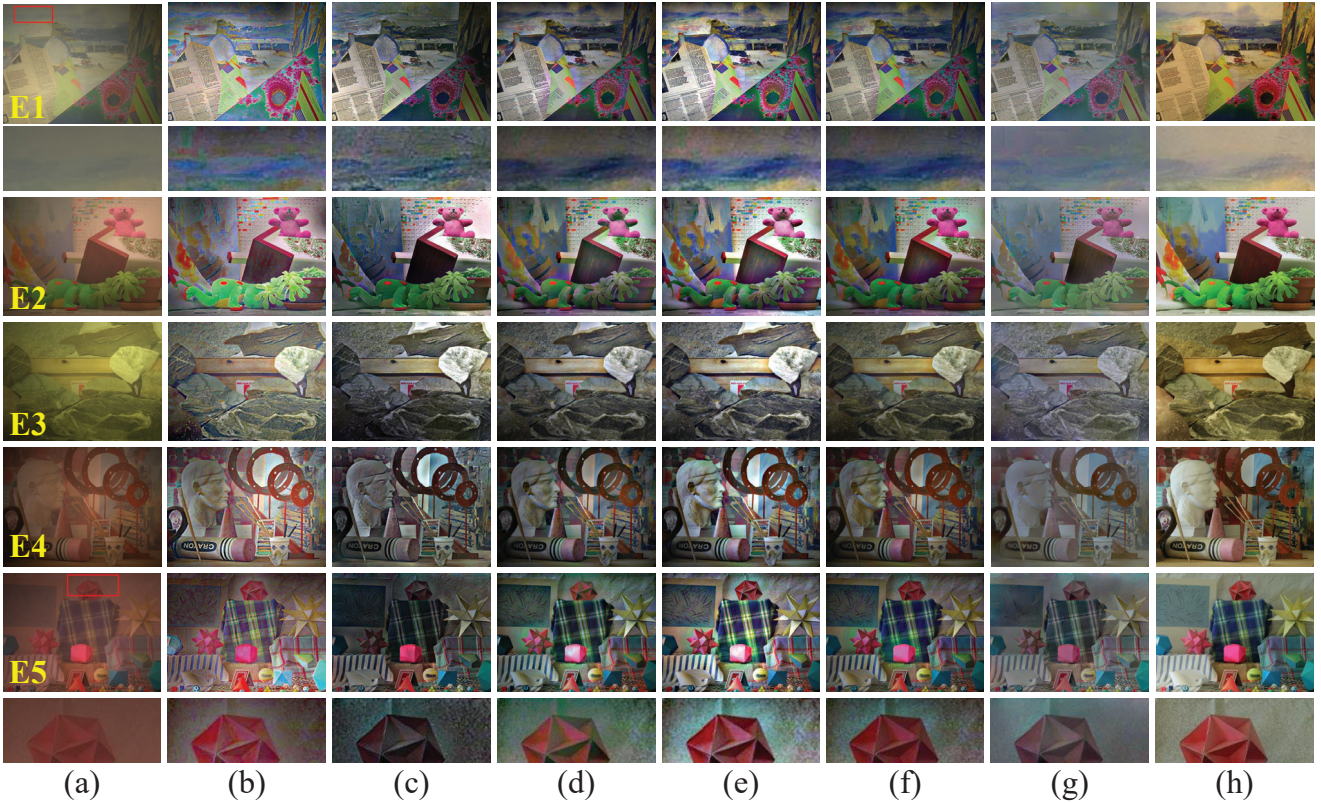


Figure 4. Comparisons of state-of-the-art nighttime dehazing methods on synthetic scenes. (a) Nighttime hazy images. (b) NDIM [40]. (c) GS [21]. (d) MRP [39]. (e) MRP-Faster [39]. (f) OSFD [41]. (g) Ours. (h) Ground truths.

noise and reveal the details.

In order to avoid the deviation of subjective evaluation, two famous full-reference metrics, peak signal-to-noise (PSNR) and structural similarity (SSIM) [33] are used for quantitative comparisons. Table 1 reveals the evaluation results on Fig. 4. From Table 1, our results achieve best scores for PSNR and SSIM, which signifies the superior dehazing performance on nighttime hazy scenes. Moreover, the dataset NHM including 350 synthetic images with different haze levels is also tested for assess the robustness of the proposed framework. By analyzing Table 2, we can conclude that the proposed method provides the best scores quantitatively and shows the best performance on synthetic dataset.

4.3. Noise Suppression

We evaluate the performance of the proposed framework in the aspect of noise suppression. Fig. 5 shows the dehazed results with different approaches. As observed in Fig. 5, the noise hidden in the low-light regions is very intensive. Although NDIM, GS, MRP, MRP-Faster and OSFD can sufficiently enhance the visibility of nighttime hazy images, the hidden noise is also amplified. Our method provides pleas-

ant dehazed results with less noise.

4.4. Ablation Study

Table 3 reveals the significance of the proposed variational decomposition model and multi-scale decomposition strategy in the proposed framework. To verify the superior of the proposed model, the weighted- ℓ_2 variational model [23] instead of our model is used in the proposed framework while keeping other operations unchanged. In addition, we replace the multi-scale decomposition with single scale for proving its effectiveness. We can intuitively observe from Table 3 that the proposed model and the devised multi-scale decomposition strategy make its own contribution to the performance of the overall nighttime dehazing framework.

4.5. Convergence Speed of Proposed Model

Fig. 6 plots the average curves of errors of our model on the synthetic dataset NHM. We can find from the curves that the proposed variational model converges within 15 iterations for the dataset NHM. The selected maximum number of iterations is sufficient to produce excellent results.

Table 1. Quantitative comparisons on synthetic nighttime hazy images in Fig. 4.

Examples	NDIM [40]		GS [21]		MRP [39]		MRP_Faster [39]		OSFD [41]		Our	
	PSNR	SSIM	PSNR	SSIM	PSNR	SSIM	PSNR	SSIM	PSNR	SSIM	PSNR	SSIM
E1	12.3621	0.6162	13.7171	0.6645	14.1856	0.7247	13.7692	0.6869	14.4284	0.7277	15.8444	0.7498
E2	14.6954	0.6829	14.9221	0.7145	14.8665	0.7400	15.8630	0.7332	14.3735	0.7488	16.6698	0.7895
E3	14.9046	0.6092	14.3896	0.6284	15.7950	0.6683	14.5727	0.6462	16.5706	0.6793	16.6678	0.6887
E4	12.9891	0.5956	14.7477	0.6447	14.0008	0.6617	14.2825	0.6465	14.1065	0.6753	15.7061	0.7013
E5	13.4413	0.6130	12.8841	0.6252	14.9017	0.6893	15.1977	0.6527	14.6146	0.6940	16.8963	0.7543

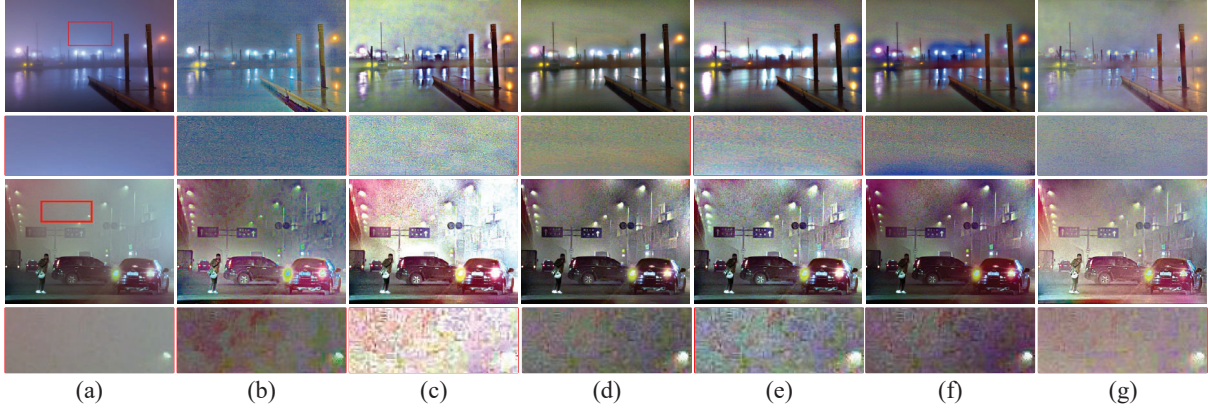


Figure 5. Comparisons of noise suppression. (a)-(g) are the input nighttime hazy images and dehazed results generated by NDIM [40], GS [21], MRP [39], MRP_Faster [39] OSFD [41] and ours, respectively.

Table 2. Quantitative comparisons on synthetic dataset NHM¹.

Methods	PSNR	SSIM
NDIM [40]	12.4924	0.5752
GS [21]	11.8963	0.5899
MRP [39]	12.9928	0.6299
MRP_Faster [39]	13.1847	0.6164
OSFD [41]	13.3027	0.6435
Our	13.6196	0.6734

Table 3. Comparisons on the dataset NHM for different variants.

Variants	w/o proposed model	w/o multi-scale strategy	Our
PSNR	13.5199	13.5792	13.6196
SSIM	0.6098	0.6706	0.6734

5. Conclusion

In this paper, we have proposed a comprehensive dehazing framework focusing on nighttime hazy images. Specifically, a novel variational decomposition model and multi-scale decomposition strategy are devised to decompose a nighttime degraded image into a base layer and two detail layers, which can simultaneously address multiple degradation issues of nighttime hazy images by using restoration and gradient manipulation operations according to differ-

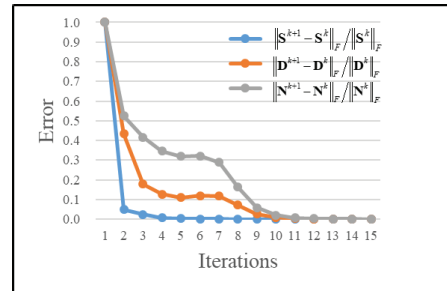


Figure 6. The average convergence curves of our model on NHM

ent attributes of image layers. Experiments verify that our nighttime dehazing framework produces pleasant dehazing results with more details and less noise, performing better than other state-of-the-art specialized nighttime dehazing approaches in both subjective and objective assessments.

6. Acknowledgments

This work was supported by Natural Science Foundation of Chongqing, China (Grant No. cstc2020jcyj-mxmxX0324) and the Construction of Chengdu-Chongqing Economic Circle Science and Technology Innovation Project (Grant No. KJCX2020007).

¹In OSFD [41], the low-light images rather than the ground truths are regarded as the reference images to compute PSNR and SSIM, resulting in higher values than the provided results in Table. 2.

References

- [1] Cosmin Ancuti, Codruta O Ancuti, Christophe De Vleeschouwer, and Alan C Bovik. Night-time dehazing by fusion. In *Proc. IEEE Int. Conf. Image Process.*, pages 2256–2260, 2016. [2](#), [3](#)
- [2] Codruta O Ancuti, Cosmin Ancuti, and Christophe De Vleeschouwer. Effective local airlight estimation for image dehazing. In *Proc. IEEE Int. Conf. Image Process.*, pages 2850–2854, 2018. [2](#), [3](#)
- [3] Dana Berman, Tali Treibitz, and Shai Avidan. Single image dehazing using haze-lines. *IEEE Transactions on Pattern Analysis and Machine Intelligence*, 2018. [1](#), [2](#), [3](#)
- [4] Trung Minh Bui and Wonha Kim. Single image dehazing using color ellipsoid prior. *IEEE Trans. Image Process.*, 27(2):999–1009, 2017. [1](#), [2](#), [3](#)
- [5] Bolun Cai, Xiangmin Xu, Kui Jia, Chunmei Qing, and Dacheng Tao. Dehazenet: An end-to-end system for single image haze removal. *IEEE Trans. Image Process.*, 25(11):5187–5198, Nov. 2016. [1](#), [2](#), [3](#)
- [6] Zeyuan Chen, Yangchao Wang, Yang Yang, and Dong Liu. PSD: principled synthetic-to-real dehazing guided by physical priors. In *IEEE Conference on Computer Vision and Pattern Recognition*, pages 7180–7189, 2021. [1](#), [2](#), [3](#)
- [7] Hang Dong, Jinshan Pan, Lei Xiang, Zhe Hu, Xinyi Zhang, Fei Wang, and Ming-Hsuan Yang. Multi-scale boosted dehazing network with dense feature fusion. In *IEEE Conference on Computer Vision and Pattern Recognition*, pages 2154–2164, 2020. [1](#), [2](#), [3](#)
- [8] Raanan Fattal. Dehazing using color-lines. *ACM Trans. Graph.*, 34(1):13:1–13:14, 2014. [1](#), [2](#), [3](#)
- [9] Raanan Fattal, Dani Lischinski, and Michael Werman. Gradient domain high dynamic range compression. *ACM Trans. Graph.*, 21(3):249–256, 2002. [5](#)
- [10] Kaiming He, Jian Sun, and Xiaoou Tang. Single image haze removal using dark channel prior. *IEEE Trans. Pattern Anal. Mach. Intell.*, 33(12):2341–2353, Dec. 2011. [1](#), [2](#), [3](#), [5](#)
- [11] Kaiming He, Jian Sun, and Xiaoou Tang. Guided image filtering. *IEEE Trans. Pattern Anal. Mach. Intell.*, 35(6):1397–1409, Jun. 2013. [5](#)
- [12] Renjie He, Mingyang Guan, and Changyun Wen. Scens: Simultaneous contrast enhancement and noise suppression for low-light images. *IEEE Transactions on Industrial Electronics*, 68(9):8687–8697, 2020. [4](#)
- [13] Mingye Ju, Can Ding, Charles A. Guo, Wenqi Ren, and Dacheng Tao. IDRLP: image dehazing using region line prior. *IEEE Trans. Image Process.*, 30:9043–9057, 2021. [1](#), [2](#), [3](#)
- [14] Mingye Ju, Can Ding, Y Jay Guo, and Dengyin Zhang. Idgcp: Image dehazing based on gamma correction prior. *IEEE Trans. Image Process.*, 29:3104–3118, 2019. [1](#), [2](#), [3](#)
- [15] Mingye Ju, Zhenfei Gu, and Dengyin Zhang. Single image haze removal based on the improved atmospheric scattering model. *Neurocomputing*, 260:180–191, 2017. [5](#)
- [16] Beomhyuk Koo and Gyeonghwan Kim. Nighttime haze removal with glow decomposition using GAN. In Shivakumara Palaiahnakote, Gabriella Sanniti di Baja, Liang Wang, and Wei Qi Yan, editors, *Pattern Recognition - 5th Asian Conference, ACPR*, volume 12046, pages 807–820. Springer, 2019. [3](#)
- [17] H Koschmieder. *Theorie der horizontalen Sichtweite: Kontrast und Sichtweite*. Munich, Germany: Keim & Nemnich, 1925. [1](#)
- [18] Boyi Li, Xiulian Peng, Zhangyang Wang, Jizheng Xu, and Dan Feng. Aod-net: All-in-one dehazing network. In *Proc. IEEE Conf. Comput. Vis. Pattern Recognit.*, pages 4770–4778, 2017. [1](#), [2](#), [3](#)
- [19] Runde Li, Jinshan Pan, Zechao Li, and Jinhui Tang. Single image dehazing via conditional generative adversarial network. In *Proc. IEEE Conf. Comput. Vis. Pattern Recognit.*, pages 8202–8211, 2018. [1](#), [2](#), [3](#)
- [20] Yu Li, Fangfang Guo, Robby T. Tan, and M. S. Brown. A contrast enhancement framework with jpeg artifacts suppression. In *ECCV*, 2014. [5](#)
- [21] Yu Li, Robby T Tan, and Michael S Brown. Nighttime haze removal with glow and multiple light colors. In *Proc. IEEE Int. Conf. Comput. Vision*, pages 226–234, 2015. [2](#), [3](#), [5](#), [6](#), [7](#), [8](#)
- [22] Z. Liang, J. Xu, D. Zhang, Z. Cao, and Z. Lei. A hybrid 11-10 layer decomposition model for tone mapping. In *IEEE Conference on Computer Vision and Pattern Recognition*, 2018. [4](#)
- [23] Yun Liu, Anzhi Wang, Hao Zhou, and Pengfei Jia. Single nighttime image dehazing based on image decomposition. *Signal Processing*, 183:107986, 2021. [2](#), [3](#), [5](#), [7](#)
- [24] Gaofeng Meng, Ying Wang, Jiangyong Duan, Shiming Xiang, and Chunhong Pan. Efficient image dehazing with boundary constraint and contextual regularization. In *Proceedings of the IEEE International Conference on Computer Vision*, pages 617–624, 2013. [2](#)
- [25] Zetian Mi, Huan Zhou, Yijun Zheng, and Minghui Wang. Single image dehazing via multi-scale gradient domain contrast enhancement. *IET Image Process.*, 10(3):206–214, 2016. [5](#)
- [26] Dubok Park, David K Han, and Hanseok Ko. Nighttime image dehazing with local atmospheric light and weighted entropy. In *Proc. IEEE Int. Conf. Image Process.*, pages 2261–2265, 2016. [2](#)
- [27] Soo-Chang Pei and Tzu-Yen Lee. Nighttime haze removal using color transfer pre-processing and dark channel prior. In *Proc. IEEE Int. Conf. Image Process.*, pages 957–960, 2012. [1](#), [2](#), [3](#)
- [28] Xu Qin, Zhilin Wang, Yuanchao Bai, Xiaodong Xie, and Huizhu Jia. Ffa-net: Feature fusion attention network for single image dehazing. In *The Thirty-Fourth AAAI Conference on Artificial Intelligence, AAAI*, pages 11908–11915, 2020. [1](#), [2](#), [3](#)
- [29] Yanyun Qu, Yizi Chen, Jingying Huang, and Yuan Xie. Enhanced pix2pix dehazing network. In *Proc. IEEE Conf. Comput. Vis. Pattern Recognit.*, pages 8160–8168, 2019. [1](#), [2](#), [3](#)
- [30] Wenqi Ren, Si Liu, Hua Zhang, Jinshan Pan, Xiaochun Cao, and Ming-Hsuan Yang. Single image dehazing via multi-scale convolutional neural networks. In *Proc. Eur. Conf. Comput. Vis.*, pages 154–169, 2016. [1](#), [2](#), [3](#)

- [31] Wenqi Ren, Lin Ma, Jiawei Zhang, Jinshan Pan, Xiaochun Cao, Wei Liu, and Ming-Hsuan Yang. Gated fusion network for single image dehazing. In *Proceedings of the IEEE Conference on Computer Vision and Pattern Recognition*, pages 3253–3261, 2018. 1, 2, 3
- [32] Yuanjie Shao, Lerenhan Li, Wenqi Ren, Changxin Gao, and Nong Sang. Domain adaptation for image dehazing. In *IEEE Conference on Computer Vision and Pattern Recognition*, pages 2805–2814, 2020. 1, 2, 3
- [33] Zhou Wang, Alan C Bovik, Hamid R Sheikh, Eero P Simoncelli, et al. Image quality assessment: from error visibility to structural similarity. *IEEE Trans. Image Process.*, 13(4):600–612, 2004. 7
- [34] Haiyan Wu, Yanyun Qu, Shaohui Lin, Jian Zhou, Ruizhi Qiao, Zhizhong Zhang, Yuan Xie, and Lizhuang Ma. Contrastive learning for compact single image dehazing. In *IEEE Conference on Computer Vision and Pattern Recognition*, pages 10551–10560, 2021. 1, 2, 3
- [35] Li Xu, Cewu Lu, Yi Xu, and Jiaya Jia. Image smoothing via ℓ_0 gradient minimization. *ACM Trans. Graph.*, 30(6):174:1–174:12, 2011. 4
- [36] Dong Yang and Jian Sun. Proximal dehaze-net: A prior learning-based deep network for single image dehazing. In *Proceedings of the European Conference on Computer Vision (ECCV)*, pages 702–717, 2018. 1, 2, 3
- [37] Minmin Yang, Jianchang Liu, and Zhengguo Li. Superpixel-based single nighttime image haze removal. *IEEE Trans. Multimedia*, 20(11):3008–3018, 2018. 2
- [38] Teng Yu, Kang Song, Pu Miao, Guowei Yang, Huan Yang, and Chenglizhao Chen. Nighttime single image dehazing via pixel-wise alpha blending. *IEEE Access*, 7:114619–114630, 2019. 2, 3
- [39] Jing Zhang, Yang Cao, Shuai Fang, Yu Kang, and Chang Wen Chen. Fast haze removal for nighttime image using maximum reflectance prior. In *Proc. IEEE Conf. Comput. Vis. Pattern Recognit.*, pages 7418–7426, 2017. 2, 5, 6, 7, 8
- [40] Jing Zhang, Yang Cao, and Zengfu Wang. Nighttime haze removal based on a new imaging model. In *Proc. IEEE Int. Conf. Image Process.*, pages 4557–4561, 2014. 1, 2, 3, 5, 6, 7, 8
- [41] Jing Zhang, Yang Cao, Zheng-Jun Zha, and Dacheng Tao. Nighttime dehazing with a synthetic benchmark. In *Proc. of the 28th ACM International Conference on Multimedia*, pages 2355–2363, 2020. 2, 3, 5, 6, 7, 8
- [42] Qingsong Zhu, Jiaming Mai, and Ling Shao. A fast single image haze removal algorithm using color attenuation prior. *IEEE Trans. Image Process.*, 24(11):3522–3533, Nov. 2015. 1, 2, 3